PRAMANA — journal of physics | © Indian Academy of Sciences | Vol. 53, No. 2
August 1999
pp. 289–305

Beta decay of ^{125}Sb and level structures in ^{125}Te

M SAINATH*, K VENKATARAMANIAH* and P C SOOD*,†
*Department of Physics, Sri Sathya Sai Institute of Higher Learning,
Prashanthinilayam 515 134, India
†Department of Physics, Banaras Hindu University, Varanasi 221 005, India

MS received 7 November 1998; revised 24 May 1999

Abstract. The decay of 2.76y ^{125}Sb to levels of ^{125}Te has been studied using an HPGe detector for gamma-ray and a mini orange electron spectrometer for conversion electron measurements. We identify 38 transitions in this decay, including 13 gamma rays and 4 conversion electron lines being reported for the first time. New results also include E1 multipolarity assignments to 3 newly observed transitions and M-shell conversion coefficient for the 109 keV M4 transition. A revised ^{125}Te level scheme is constructed using Ritz combination principle. While confirming the existence of 10 well established levels below 700 keV excitation, we introduce 3 other levels at 402.0, 538.6 and 652.9 keV. Interpretation of the observed levels in terms of various theoretical approaches is briefly discussed. The newly introduced 538.6 keV (1/2$^+$) and 652.9 keV (3/2$^+$) levels are seen as the two missing members of the $(s_{1/2} \otimes 2^+)$ and $(d_{3/2} \otimes 2^+)$ sextuplet in the quasiparticle-phonon coupling scheme.

Keywords. Radioactivity; ^{125}Sb beta decay; mini orange; internal conversion coefficients; multipolarity; ^{125}Te level scheme.

PACS Nos 23.20.Lv; 23.20.Nx; 27.60.+j

1. Introduction

Level scheme of the near-magic nuclide $^{125}_{52}$Te$_{73}$ has been extensively investigated over the past fifty years using a wide variety of experimental techniques [1,2]. Low-energy excitation spectrum of this nucleus is mainly governed by neutrons in the half-filled $N = 65-82$ configuration space ($s_{1/2}, d_{3/2}, h_{11/2}$ orbitals) and, at medium energies, the core excitations from the $g_{7/2}, d_{5/2}$ filled orbitals. Detailed information on the level structures upto excitation energy of 700 keV has been sought through gamma-ray and conversion electron spectroscopy following beta decay of the long-lived ($t_{1/2}$ = 2.76y) source ^{125}Sb [3–22]. Supporting information, albeit with lesser precision, over this region has come from a variety of other techniques [1,2,23–28], e.g. ^{125}I EC decay, radiative neutron capture, Coulomb excitation, $(\alpha, xn\gamma)$ in-beam experiments, particle transfer reaction studies etc. Several theoretical approaches [13,21,28–34], e.g., many-particle shell model, quasiparticle-phonon coupling (QPC) model, interacting boson–fermion model (IBFM) etc., have been pursued to interpret the observed data. However, in spite of these longcontinued investigations, a number of open questions still persist even in the low-energy spectrum. The significant questions, which need to be addressed to, include (i) search for certain expected (from reaction data or from model considerations) levels which are as yet unobserved in decay studies; (ii) careful spectroscopic investigations to examine the evidence for unconfirmed or disputed levels; (iii) particular attention to identify relatively weaker transitions; (iv) a focussed study of the high-multipole (M4) transition in ^{125}Sb decay process, and (v) an exhaustive and careful study of the conversion electron spectra to clear the reported uncertainties. These questions are described more specifically in the following paragraphs.

A low-lying $1/2^+$ state, expected from systematics and also from theoretical considerations, is indicated around 538 keV from single-particle transfer reaction studies [27], but it still remains unobserved in decay or any other studies [1,13]. Also, the possible existence of 402 keV and 653 keV levels, tentatively proposed in early decay studies [4–6,9], was not confirmed in later experiments [1]. One of the main reasons for the situation is the fact that the beta-decaying source ^{125}Sb is one of the internationally adopted gamma-ray energy and intensity standards for calibration of Ge detectors [2,19,35] and, more recently, also as an analytical instrumentation standard in fuel reprocessing [20]. This factor has caused major attention to be focussed mainly on relatively stronger transitions in this decay, whereas confirmation of the disputed levels requires focus on the weaker transitions. The $11/2^-$ isomer decays by a high-multipole M4 transition; however, as given in the nuclear data sheets [1] data sets, this M4 transition does not appear in several reports of spectroscopic studies following ^{125}Sb decay. In our study, we aim to pay special attention to this transition as well.

A close look at the earlier conversion electron measurements [4,6,7,11,22] also reveals a similar situation. Mazets and Sergeenkov [7], using a high resolution prism-type β-spectrometer, obtained data for $20K$- and $8L$-conversion lines and deduced multipolarities for 10 transitions, based on relative intensities, K/L ratios and L-subshell ratios. Other earlier [4,6] as well as later [11,22] reports include results for barely half this number. Further, Goswamy *et al* [22], in a recent study with a mini-orange electron spectrometer aimed at ‘standardization of a few commonly available radioisotopes as conversion electron calibration sources’, remarked that the conversion electron intensity results of Mazets and Sergeenkov [7] ‘have significantly large uncertainties even for strong conversion lines’. Accordingly, a careful reinvestigation of the complete conversion electron spectrum of ^{125}Sb decay is called for.

In the present study we address these questions through precision measurements of gamma-ray energies and relative intensities using a HPGe detector and similar measurements for conversion electrons from ^{125}Sb decay using a mini-orange electron spectrometer. In §2, we briefly describe the experimental set-up, which is essentially the same as employed in our earlier study of ^{147}Nd decay [36]. Section 3 includes the results of our measurements and the deduced ^{125}Te level scheme, along with a brief discussion of its interpretation in terms of various theoretical approaches. Summary and conclusions of our study are given in the final section. Some of these results have been briefly reported earlier [37,38].

2. Experimental procedure

The carrier-free sample of the radioactive source ^{125}Sb prepared by thermal neutron irradiation of ^{125}Sn, was obtained from Bhabha Atomic Research Centre, Mumbai, in liquid form as antimony chloride in dilute HCl solution. The ^{125}Sb source was allowed to decay for about 8 months, mainly to achieve two purposes. (i) It purified the source of any short-lived impurities and (ii) it allowed the $11/2^-$ 144 keV isomeric level in ^{125}Te, with a half life of 58 days, to be reasonably well populated with a view to properly investigate its 109 keV high multipole (M4) decay transition. Sources required for acquiring spectra were prepared by drying the source solution on aluminised mylar foils supported by thin aluminum discs of 1.0 cm diameter. The count rate was kept at around 500 counts/sec. Sources required for conversion electron spectroscopy were specially made very thin to avoid backscattering and absorption of the electrons in the source.

Singles gamma spectra were recorded with a 60 cc HPGe detector (FWHM = 665 eV at 5.9 keV (^{55}Fe) and 1.80 keV at 1.33 MeV (^{60}Co)) coupled to a 4K PC based multichannel analyser. Gamma singles spectra were acquired at a source-detector distance of 25 cm. Counting period lasted on an average of 4.5×10^5 seconds per spectrum. Efficiency calibration for the HPGe detector was done using standard radioactive sources. The low energy 19.80 keV spectrum was acquired using a Si(Li) detector (FWHM = 190 eV at 5.9 keV (^{55}Fe)). The gamma ray peaks were analysed using the computer code FIT [39].

The conversion electron measurements employed a mini-orange spectrometer comprising of (i) a windowless Si(Li) detector (surface area = 78 mm^2, sensitive depth = 5.3 mm, FWHM = 1 keV at 115 keV and 2.3 keV at 624.5 keV), and (ii) a mini-orange filter composed of nine thin wedge-shaped permanent magnets fixed in an orange array in a circular brass frame of 16.2 cm diameter, with a central absorber made of lead to prevent direct exposure of the Si(Li) to photons from the source. A clean vacuum of about 10^{-7} mbar was maintained. The transmission curve was optimized using a ^{131}Ba source for the best transmission over the electron energies from 40 keV to 800 keV at a source-to-magnet distance of 7.5 cm and a magnet-to-detector distance of 4.5 cm. Optimization for the low-energy (10–100 keV) region was done by using a ^{153}Gd source.

Our determination of internal conversion coefficients (ICC's) employs normalized-peak-to-gamma (NPG) method using the relative conversion electron and gamma-ray intensities normalized via the conversion coefficient of the intense 428 keV transition. The multipolarities of various transitions were derived from comparison of our data with the tables of Hager and Seltzer [40].

3. Results and discussion

Now we present the results of our gamma-ray and conversion electron measurements and discuss the placement of the observed transitions in a revised level scheme of ^{125}Te.

3.1 Gamma-ray and conversion-electron transitions

Our typical gamma spectra are shown in figures 1a–g. We employ the 'comparison with benchmark' test to establish the credibility of our identification of as-yet unconfirmed weaker transitions and their precise energies. The most recent (IAEA-1995) energy calibration standards [2,35] are compared with our results in table 1a; a similar comparison with the 8 additional transitions included in the 'standardization' analysis of Helmer [19] is

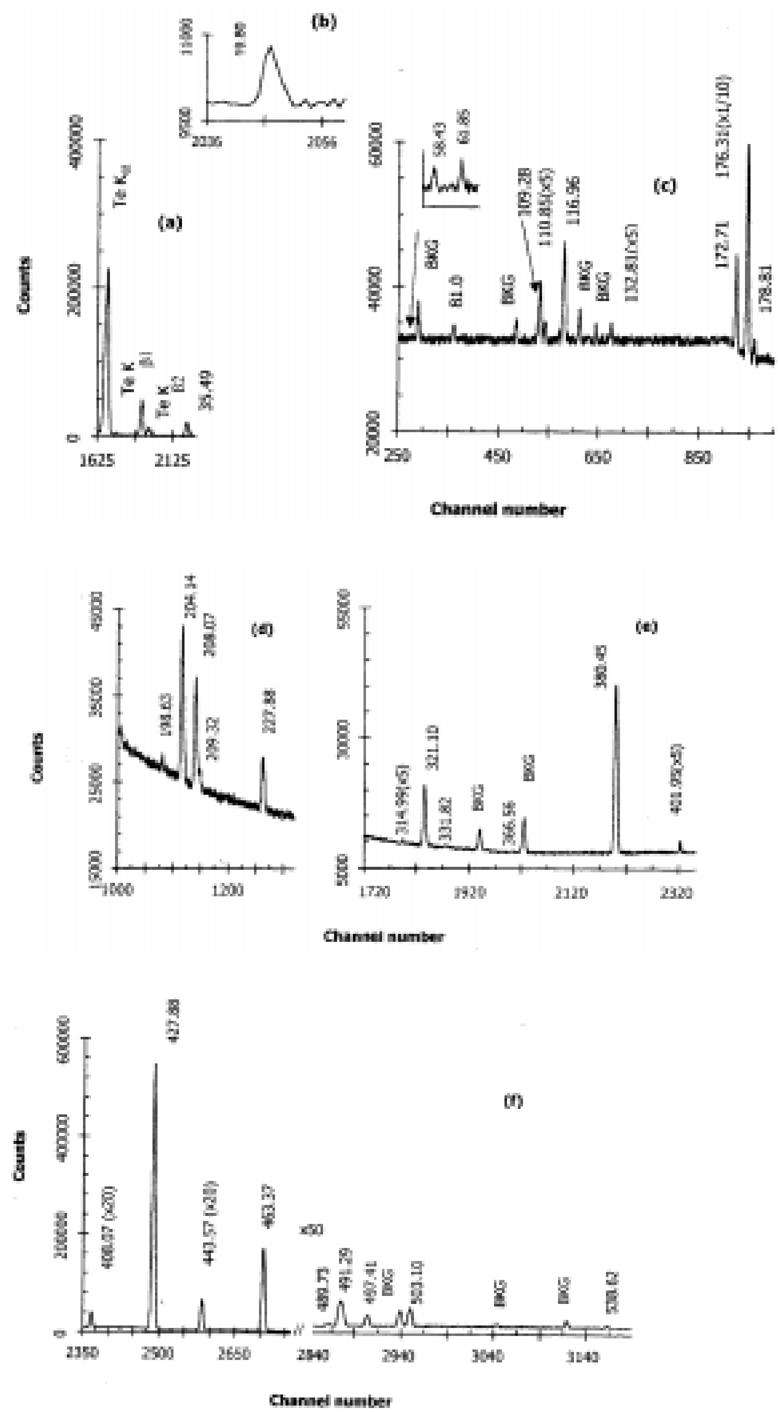

Figure 1(a–f).

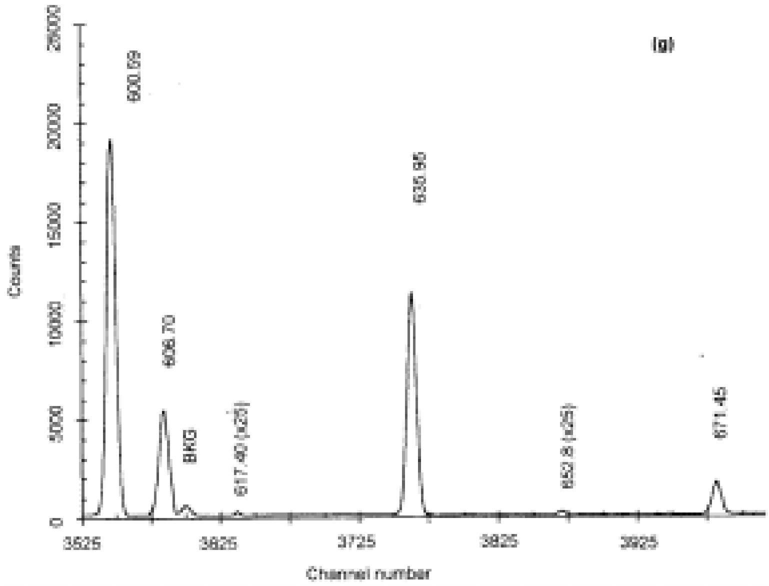

Figure 1(a–g). Single γ-ray spectra observed following the β-decay of ^{125}Sb recorded by a 60 cc. HPGe detector. The peaks labelled BKG arise from other sources.

Table 1. Comparison of our (SVS) measured gamma energies with (a) the corresponding values for the transitions adopted as international (IAEA-95) gamma energy calibration standards [35] and (b) other gamma energies precisely determined in 'standardization' studies by Helmer-90 [19] in the decay of ^{125}Sb. Numbers within the parentheses denote the uncertainties in the last digit(s).

Gamma energies (keV)			
SVS	(a) IAEA - 95	SVS	(b) Helmer-90
176.308(2)	176.314(2)	35.489(4)	35.489(5)
380.454(8)	380.454(8)*	172.708(7)	172.719(8)
427.880(5)	427.874(4)	198.631(14)	198.654(11)
463.368(4)	463.365(4)	204.144(8)	204.139(8)
600.589(3)	600.597(2)	208.074(10)	208.079(4)
606.700(2)	606.713(2)	227.876(10)	227.891(10)
635.951(3)	635.950(3)	408.069(12)	408.065(10)
671.445(6)	671.441(6)	443.565(7)	443.554(9)

*Taken from ref. [19].

presented in table 1b. It is seen that almost in all cases the deviations are comparable to the assigned uncertainties; the average deviation for the 16 transition energies is less than 8 eV. This excellent agreement of our measured gamma energies and the adopted 'benchmark' values in the IAEA calibration standard tables and other similar standardization measurements provides us with a firm basis for the identification of new transitions and also for the

Table 2. Gamma energies and relative gamma intensities of the transitions observed in decay of ^{125}Sb are listed in comparison with earlier reports. The earlier reports include Longo-90 [18], Helmer-90 [19], Fawwaz-93 [21] and NDS-93 [1]. Our results are under the heading SVS. The last column lists the rounded off level energies and assigned spin-parities of the initial and final levels in each case.

	I_γ					
E_γ (keV)	Longo-90	Helmer-90	Fawwaz-93	NDS-93	SVS	$E_i(I_i^\pi) \rightarrow E_f(I_f^\pi)$
19.80(6)	0.068(3)		0.072(6)	0.068(2)	0.068(3)	463(5/2$^+$) → 444(3/2$^+$)
35.489(4)	14.53(35)		14.79(8)	14.5(4)	17.7(2)	36(3/2$^+$) → 0(1/2$^+$)
58.43(5)$^{(a)}$			0.093(2)	0.091(4)	0.0042(20)	
61.85(16)					0.0068(27)	525(7/2$^-$) →463(5/2$^+$)
81.02(4)					0.017(1)	402(7/2$^+$) →321(9/2$^-$)
109.28(4)	0.233(5)		0.235(16)	0.274(9)	0.232(6)	145(11/2$^-$) →36(3/2$^+$)
110.85(9)	0.0036(6)			0.0036(2)	0.0039(3)	636(7/2$^+$) →525(7/2$^-$)
116.956(10)	1.03(4)	0.867(24)	0.885(5)	0.961(5)	0.945(15)	642(7/2$^+$) →525(7/2$^-$)
132.81(14)					0.0029(19)	672(5/2$^+$) →539(1/2$^+$)
172.708(8)	0.75(5)	0.659(11)	0.72(4)	0.67(4)	0.67(4)	636(7/2$^+$) →463(5/2$^+$)
176.308(2)	23.06(14)	22.96(24)	23.65(34)	23.05(8)	23.09(20)	321(9/2$^-$) →145(11/2$^-$)
178.814(7)	0.110(9)		0.099(6)	0.097(8)	0.121(2)	642(7/2$^+$) →463(5/2$^+$)
198.631(14)	0.054(11)		0.046(9)	0.046(5)	0.044(3)	642(7/2$^+$) →444(3/2$^+$)
204.144(8)	1.105(11)	1.080(23)	1.19(5)	1.102(8)	1.014(10)	525(7/2$^-$) →321(9/2$^-$)
208.074(10)	0.808(9)	0.825(16)	0.89(4)	0.814(11)	0.860(10)	672(5/2$^+$) →463(5/2$^+$)
209.32(9)					0.152(9)	653$^{(b)}$ →444(3/2$^+$)
227.876(10)	0.437(8)	0.443(23)	0.465(25)	0.440(7)	0.442(9)	672(5/2$^+$) →444(3/2$^+$)
314.99(11)	0.0138(9)			0.0132(14)	0.0144(15)	636(7/2$^+$) →321(9/2$^-$)
321.101(2)	1.40(2)	1.41(3)	1.45(5)	1.387(9)	1.43(2)	642(7/2$^+$) →321(9/2$^-$)
331.82(6)					0.0085(8)	653$^{(b)}$ →321(9/2$^-$)
366.56(11)					0.027(2)	402(7/2$^+$) →36(3/2$^+$)
380.454(8)	5.13(4)	5.14(5)	5.09(3)	5.12(4)	5.17(4)	525(7/2$^-$) →145(11/2$^-$)
401.95(12)					0.021(2)	402(7/2$^+$) →0(1/2$^+$)
408.069(12)	0.611(12)	0.630(19)	0.59(2)	0.621(10)	0.624(7)	444(3/2$^+$) →36(3/2$^+$)
427.880(5)	100	100	100	100	100	463(5/2$^+$) →36(3/2$^+$)
443.565(7)	1.03(2)	1.019(29)	1.03(1)	1.019(11)	1.051(11)	444(3/2$^+$) →0(1/2$^+$)
463.368(4)	35.47(5)	35.07(28)	35.64(10)	35.45(5)	35.12(18)	463(5/2$^+$) →0(1/2$^+$)
489.73(8)					0.0046(23)	525(7/2$^-$) →36(3/2$^+$)
491.29(14)					0.016(8)	636(7/2$^+$) →145(11/2$^-$)
497.41(14)	0.013(2)		0.018(3)	0.029(13)	0.009(1)	642(7/2$^+$) →145(11/2$^-$)
503.10(6)					0.013(6)	539(1/2$^+$) →36(3/2$^+$)
538.62(12)					0.0047(25)	539(1/2$^+$) →0(1/2$^+$)
600.589(3)	60.36(11)	59.09(45)	59.70(10)	60.35(17)	59.22(18)	636(7/2$^+$) →36(3/2$^+$)
606.700(2)	17.03(3)	16.70(14)	16.98(7)	16.98(7)	16.92(6)	642(7/2$^+$) →36(3/2$^+$)
617.40(14)					0.018(2)	653$^{(b)}$ →36(3/2$^+$)
635.951(3)	38.36(15)	35.72(30)	38.78(32)	38.2(3)	38.32(12)	672(5/2$^+$) →36(3/2$^+$)
652.8(4)					0.009(3)	653$^{(b)}$ →0(1/2$^+$)
671.445(6)	6.06(2)	6.05(6)	5.97(11)	6.06(2)	6.03(2)	672(5/2$^+$) →0(1/2$^+$)

$^{(a)}$Not placed in the level scheme.
$^{(b)}$The spin-parity of the 653 keV level could be (3/2,5/2)$^+$, with the 3/2$^+$ assignment favoured from model considerations discussed in the text.

use of our measured gamma energies to arrive at a revised level scheme for ^{125}Te through application of Ritz combination principle.

A complete listing of the energies and the relative intensities of the 38 gamma transitions, observed in our study and shown in figures 1a–g, is given in table 2. In addition to a comparison of our (SVS) intensity values with NDS-93 [1] and Helmer [19], we also include the results from a post-NDS-93 HPGe study by Fawwaz and Stewart [21] and the comprehensive report by Longoria-Gandara *et al* [18]; the latter report includes a tabulation of the relative intensities given by seven other pre-1990 investigators. In accordance with the usual convention, the gamma intensities in table 2 are quoted relative to the intense 427.88 keV (assumed I_γ = 100) transition. We do not see the 146 keV transition reported in a number of earlier studies [13,18]. On the other hand, we observe 13 gamma transitions not given in NDS-93 or any other report included in table 2; a few of these additional gammas had earlier been tentatively suggested [4–6,15], but they do not appear in the evaluated data set of NDS-93. The last column in table 2 gives the placement of each transition between ^{125}Te levels, as discussed later in this section. Only one gamma transition (58.43 keV), out of the 38 gammas listed in table 2, has not been placed in the ^{125}Te level scheme.

Typical conversion electron spectra from our study are shown in figures 2a–c. Conversion electron intensities and internal conversion coefficients, determined by combining the $I_{\rm ce}$ with I_γ of table 2, are listed in table 3 for the K-shell and in table 4 for the L-shell lines, in comparison with the corresponding values from the earlier reports. As mentioned in the preceding section, we employ the NPG method for determining the conversion coefficients, using the 427.88 keV transition as the standard for normalization with the adopted value of $\alpha_K(427) = 0.0111(4)$ and its M1-E2 mixing ratio of $|\delta| = 0.538(11)$ [1]. The multipolarity of each transition is then deduced from a comparison of our α_K values with the theoretical predictions for possible multipole transitions interpolated from the tables of Hager and Seltzer [40]. A determination of the K-shell ICC for the 35.5 keV transition is difficult due to low energy ($\approx$ 4 keV) of the K-electrons; in view of this constraint, multipolarity of the 35.5 keV transition has been deduced from a comparison of the α_L values. Another feature of our experiment, as mentioned in the preceding section, is to ensure that the 144 keV 11/2$^-$ isomeric state is reasonably well-populated with a view to

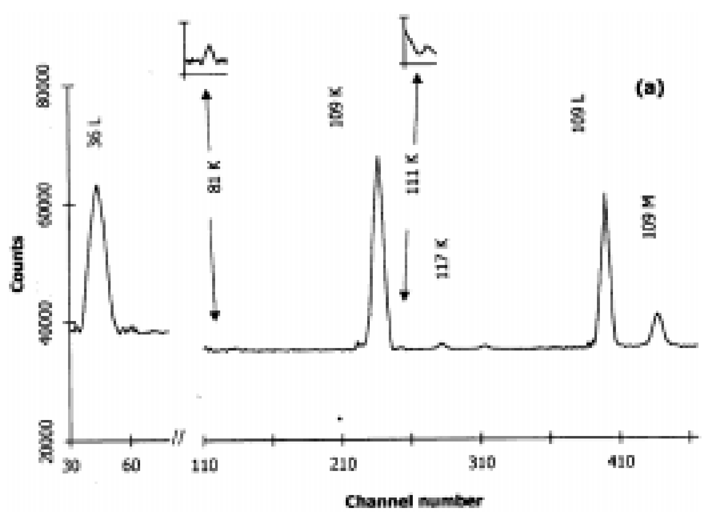

Figure 2(a).

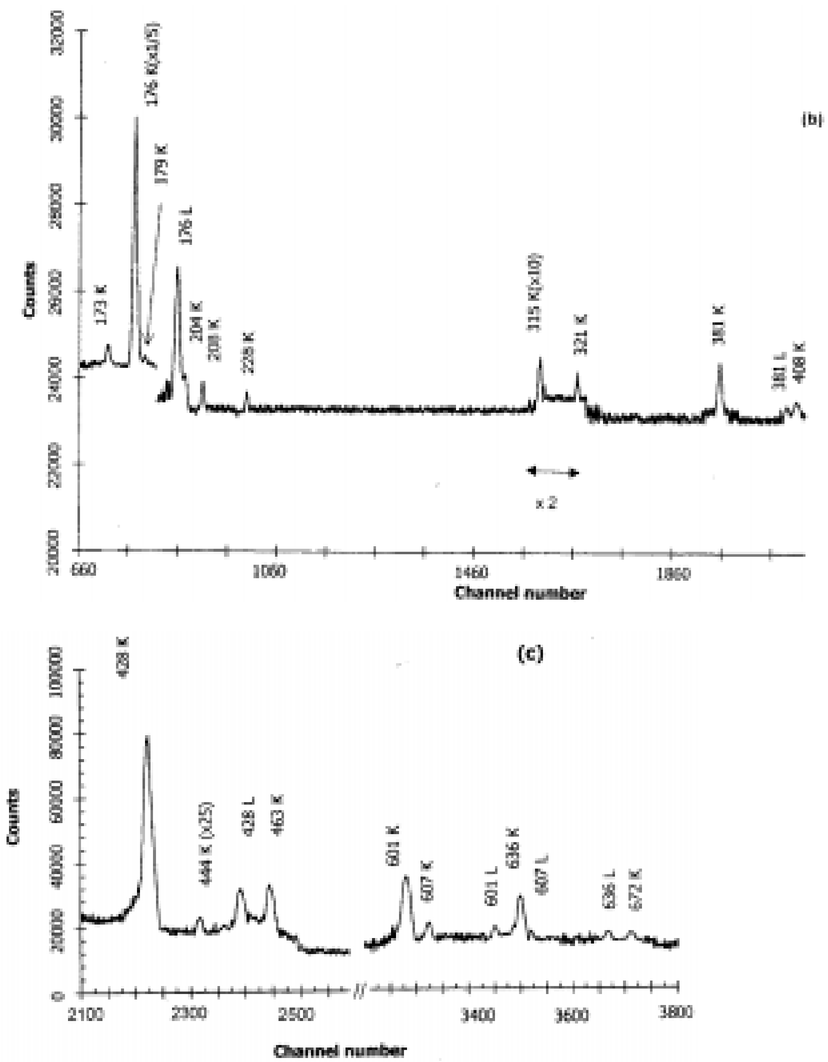

Figure 2(a–c). Internal conversion spectra following the β-decay of ^{125}Sb taken with mini orange spectrometer.

establish the properties of the 109 keV high-multipole (M4) transition. As seen in figure 2a, we not only have distinct 109 keV K and L lines but the M-line is also clearly seen in our electron spectrum. Our value of $\alpha_M = 22.4(18)$ compares well with the theoretical value of 24 for an M4 transition from Hager and Seltzer tables [40]. This M4 transition is discussed in more detail in another publication [37].

3.2 Revised ^{125}Te level scheme

Using the precisely determined transition energies as input data for application of the Ritz combination principle, we now proceed to construct the ^{125}Te level scheme. The

Table 3. K-conversion electron data from the decay of ^{125}Sb. The respective columns from the left list the transition energies in ^{125}Te, relative K-conversion electron intensities determined by Mazets and Sergeenkov [7], Goswamy *et al* [22], and in the present experiment (labelled SVS), the internal conversion coefficients α_K from the nuclear data sheets NDS-93 [1], Fawwaz and Stewart [21] and SVS, and our deduced multipolarities in comparison with the adopted multipolarities in NDS-93 [1].

	$I_{\rm ce}$ (K)			ICC (α_K)			Multipolarity	
E_γ (keV)	Mazets	Goswamy	SVS	NDS-93	Fawwaz	SVS	NDS-93	SVS
81.02(4)			0.70(15)			0.45(10)		E1
109.28(4)			3514(168)	169(7)$^{(a)}$		166(11)	M4	M4
110.85(9)	10(3)$^{(b)}$		0.34(6)			0.96(19)		(E1)
116.956(10)	6.2(7)		6.4(8)	0.074(9)	0.075(15)	0.075(10)	(E1)	E1
172.708(8)	5.4(5)		5.5(8)	0.092(11)	0.080(15)	0.091(14)	M1+E2	M1+E2
176.308(2)	260(15)		297(15)	0.129(10)		0.142(9)	M1+E2	M1+E2
178.814(7)	2.0(5)		1.3(2)	0.24(6)	0.215(65)	0.12(2)		M1+E2
204.144(8)	7.8(4)		9.7(6)	0.081(6)		0.105(8)	M1+E2	M1+E2
208.074(10)	6.5(4)		6.1(4)	0.092(5)	0.078(14)	0.078(6)	M1+E2	M1+E2
227.876(10)	3.3(5)		4.0(2)	0.086(14)	0.075(17)	0.099(7)	(M1+E2)	M1+E2
314.99(11)	–		0.051(9)			0.039(8)		(E1)
321.101(2)	1.3(4)		1.34(8)	0.011(3)	0.0095(30)	0.0103(7)	E1	E1
380.454(8)	6.1(6)	6.2(6)	6.5(3)	0.0138(8)		0.0138(8)	(E2)	E2
408.069(12)	0.9(2)	0.55(6)	0.92(6)	0.0107(19)	0.016(4)	0.0164(11)	M1+E2	M1+E2
427.880(5)	100	100	100	0.0111(18)	0.011(2)	0.0111(4)	M1+E2	M1+E2
443.565(7)	1.2(3)	0.9(2)	0.99(7)	0.014(7)	0.012(4)	0.0104(9)	M1+E2	M1+E2
463.368(4)	26.7(10)		26.9(10)	0.00864()	0.0086(2)	0.0084(4)	E2	E2
600.589(3)	21.7(4)		22.2(10)	0.00425(10)	0.0040(6)	0.0042(2)	E2	E2
606.700(2)	5.6(5)	5.6(3)	5.8(3)	0.0037(3)	0.0035(7)	0.0038(2)	E2	E2
635.951(3)	13.3(7)	14.5(6)	14.6(7)	0.0042(2)	0.0036(6)	0.0042(3)	M1+E2	M1+E2
671.445(6)	1.7(3)		1.82(10)	0.0032(3)	0.0030(7)	0.0033(2)	E2	E2

$^{(a)}$The ICC for the 109 keV transition has not been listed under data from ^{125}Sb decay in NDS-93 [1].
$^{(b)}$A part of the indicated intensity could be due to the 109 keV K-conversion line.

transition multipolarities, deduced by combining the gamma and the conversion electron data, are used to confirm the spin-parity assignments to the respective levels. Well-established undisputed features of this level scheme, as seen in the latest nuclear data sheets (NDS-93) [1], are used as cross-checks in our procedure. Application of the energy sum rule in different loops leads us to the proper placement of the observed transitions and to an evaluation of the level energies in the thus constructed level scheme. The results of this exercise are shown in figure 3 which incorporates 37, out of a total of 38, observed transitions in comparison with the 23 gammas placed in the adopted level scheme of NDS-93 [1]. In common with NDS-93, the 58 keV gamma is not placed in this level scheme. The 693 keV and the 729.8 keV gammas, listed but not placed in NDS-93, lie beyond our range of observation, which is limited by the use of 4K multichannel analyser.

All the 7 positive-parity and the 3 negative-parity levels in the adopted scheme of NDS-93 appear in our level scheme with the excitation energy and the spin-parity assignment agreeing in each case. Our level scheme includes 3 additional levels with excitation energies 402.03, 538.61 and 652.87 keV; 10 out of the 13 new gammas identified by us pertain to these levels. Further, we deduce E1 multipolarity for the 81 keV, 111 keV and 315 keV

Table 4. L-shell conversion electron data from the decay of ^{125}Sb. Our measured intensities (SVS) are compared with earlier results from Mazets and Sergeenkov [7] and Goswamy *et al* [22]. The last column gives values of α_L derived from our data.

	$I_{ce}(L)$			
E_γ (keV)	Mazets	Goswamy	SVS	ICC (α_L)
35.489(4)			2264(160)	1.4(1)$^{(a)}$
109.28(4)			2450(128)	116(8)
176.308(2)	43(1)		45(3)	0.021(2)
380.454(8)	1.02(2)	1.0(1)	0.92(7)	0.00196(17)
427.880(5)	14.0(7)	12.3(5)	15.6(6)	0.00172(9)
463.368(4)	3.8(3)	3.5(2)	3.7(2)	0.00116(7)
600.589(3)	3.2(4)	2.7(2)	3.1(2)	0.00058(4)
606.700(2)	0.9(2)		1.00(8)	0.00065(6)
635.951(3)	1.8(2)	1.73(7)	2.02(13)	0.00058(4)

$^{(a)}$We determine multipolarity of the 35.489 keV transition to be M1+E2 based on this α_L value.

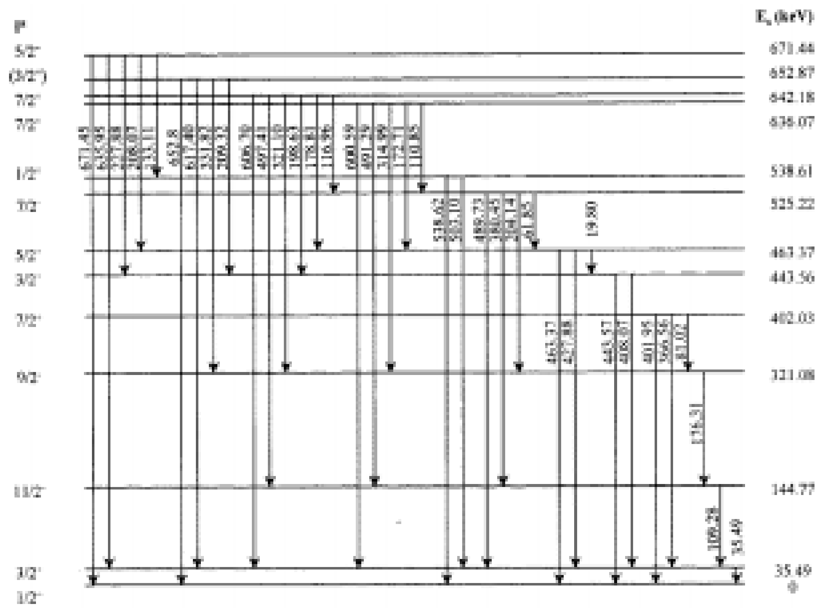

Figure 3. Level scheme of ^{125}Te deduced from the gamma and conversion electron spectra measurements following ^{125}Sb beta decay. The labelling on the left is that of the level spin and its parity, while that on the right is level energy (in keV) deduced from the transition energies listed in table 2 and the energy sum rule at each level.

transitions which had no assigned multipolarity in earlier studies. Also, the 179 keV transition is newly assigned the (M1+E2) multipolarity. In the following sections, we discuss the basis of the three newly-introduced levels.

538 keV $1/2^+$ *Level:* Consideration of the level systematics of neighboring odd-A Te isotopes, and also of the predictions of the coupling schemes applicable to these nuclei, leads one to expect a low-lying $1/2^+$ level in ^{125}Te. Based on systematics, Walters and Meyer [13] placed this level at approximately 560 keV and accordingly searched the Compton suppression spectra in the 515–535 keV region to look for its decay gamma-ray to the 35 keV level; no positive evidence for any $1/2^+$ level at (560 $\pm$ 10) keV could result from this search. Later, the single-particle transfer reaction studies of Rodland *et al* [27] indicated a tentative $I = 0$ peak at (538 $\pm$ 5) keV in the ^{126}Te (d, t) spectrum. Guided by this observation, we focussed our attention on the related energy region and identified three new gamma rays with energies 132.81, 503.10 and 538.62 keV leading to the following energy loops:

(i) The 671.44 ($5/2^+$) level decays by a 132.81 keV gamma yielding the daughter at 538.63 keV.

(ii) The decay gamma of 503.10 keV from the new level to 35.49 keV ($3/2^+$) yields a level energy of 538.59 keV

(iii) The decay gamma of 538.62 keV to the $1/2^+$ ground state gives the level energy of 538.62 keV.

In view of these results, and the $I = 0$ character from (d, t) study [27], we introduce the 538.61 keV $1/2^+$ level in our level scheme of figure 3.

653 keV $(3/2, 5/2)^+$ *Level:* Very early (1958) high-resolution spectrometer measurements of ^{125}Sb decay by Narcisi [4] had introduced two levels at 640 keV and 652 keV in ^{125}Te between the already established levels at 633 keV and 668 keV; this proposal was supported by Mann *et al* [6], who suggested $I^{\pi} = 5/2^+$ or $3/2^-$ for the 652 keV level based on α_K with 'wide error limits'. Mazets and Sergeenkov [7] were unable to detect a transition in the vicinity of 652 keV and remarked that 'the K-conversion line of such a transition would have been detected if its intensity exceeded 0.1% of that of the K 427.95 line'. No further mention of this level is made in any later study. Within our framework of looking for weak transitions with precise energy measurements, we search for the evidence of a level in ^{125}Te in the vicinity of 652 keV. We identify 4 new gammas in our spectrum with energies of 652.8 keV, 617.40 keV, 331.82 keV and 209.32 keV. These gammas have been placed in our level scheme of figure 3 as decay transitions from the newly introduced level at 652.87 keV respectively to the $1/2^+$ ground state, 35.49 keV $3/2^+$, 321.07 keV $9/2^-$ and 443.56 keV $3/2^+$ levels. All the four energy loops add up to the same summed energy, justifying their placement. However, none of these transitions could be assigned a specific multipolarity in the absence of any conversion line seen in our experiment. Thus, the spin-parity assignment for this level may be $3/2^+$ or $5/2^+$; level systematics in the neighbouring isotopes and theoretical considerations discussed later support a $3/2^+$ assignment.

402 keV $7/2^+$ *Level:* Chandra and Pandharipande [5], in their gamma–gamma coincidence experiment, observed a 80–123 keV gamma ray cascade which was tentatively suggested to correspond to the 524 keV $(7/2, 9/2)^- \xrightarrow{123} 401$ keV (?) $\xrightarrow{80}$ 321 keV $9/2^-$ decay sequence in ^{125}Te. Mann *et al* [6] could not verify this suggestion since 'these transitions lie in the regions that we cannot examine with any confidence'. Mazets and Sergeenkov [7], however, placed this cascade in the $525 \xrightarrow{82} 443 \xrightarrow{122} 321$ sequence, thus negating the existence of a level at 401 keV; this interpretation was also supported by Inamura [9]. On the other hand, Prasad [15] observed the 122–402 keV coincidence in the 525 keV sum gated coincidence spectrum and also the 122–366 keV coincidence in the 489 keV sum coincidence spectrum, thus establishing the 402 keV level with the 81 keV, 366 keV and 402 keV decay transitions respectively to the 321 keV (9/2$^-$), 35.5 keV (3/2$^+$) and the ground state (1/2$^+$) levels. None of these transitions have since been confirmed, nor do they appear in the NDS-93 adopted gammas. Our careful investigation of weak transitions identifies all three gamma rays, although we could not unambiguously see the 122 keV transition. Our energy sum-rule approach thus supports a level at 402.03 keV with these 3 decay gammas. Further, we also observe the K-conversion line for the 81 keV transition. Our evaluation of α_K for this line leads to an E1 character for the 81 keV transition and thus a possible $I^\pi = 7/2^+$ assignment for the 402 keV level in ^{125}Te.

3.3 Level systematics and model description

The near-magic $(Z = 52)$ Te isotopes with $A = 117 - 134$ correspond to the complete sequence of $N = 65 - 82$ nuclei which span the $(s_{1/2}, d_{3/2}, h_{11/2})$ configuration space beyond the $N = 64$ sub-shell closure. The three lowest energy levels (all below 400 keV) are observed to have spin-parity $I^\pi = 1/2^+, 3/2^+, 11/2^-$ in each one of the 9 odd-mass isotopes; the $11/2^-$ state occurs as a long-lived isomer in each case corresponding to the odd-particle occupying the unique parity $h_{11/2}$ orbital. The nuclide ^{125}Te under discussion lies exactly half-way across this domain. With a view to discuss the level systematics, we present in figure 4 the observed levels, with specified spin-parity and upto 1 MeV excitation, for the two stable ^{123}Te and ^{125}Te isotopes and another neighbour on either side. The positive and the negative parity levels are shown respectively in figure 4a and

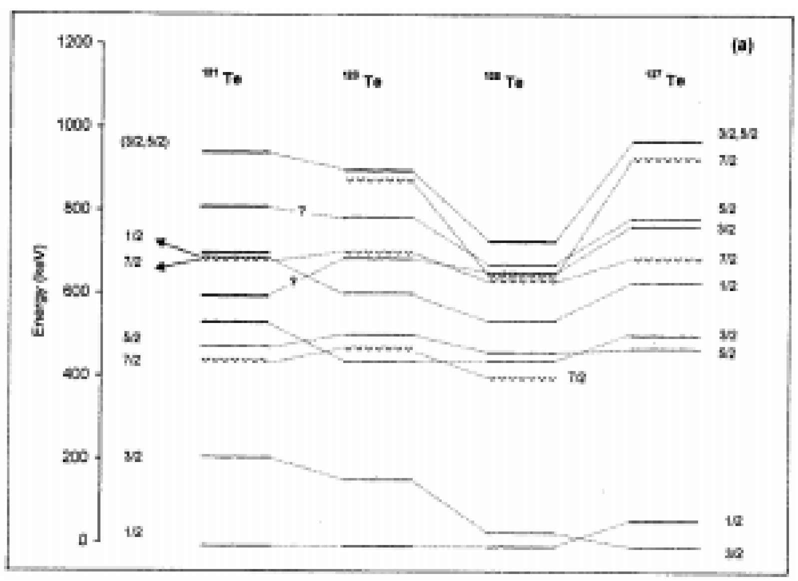

Figure 4(a).

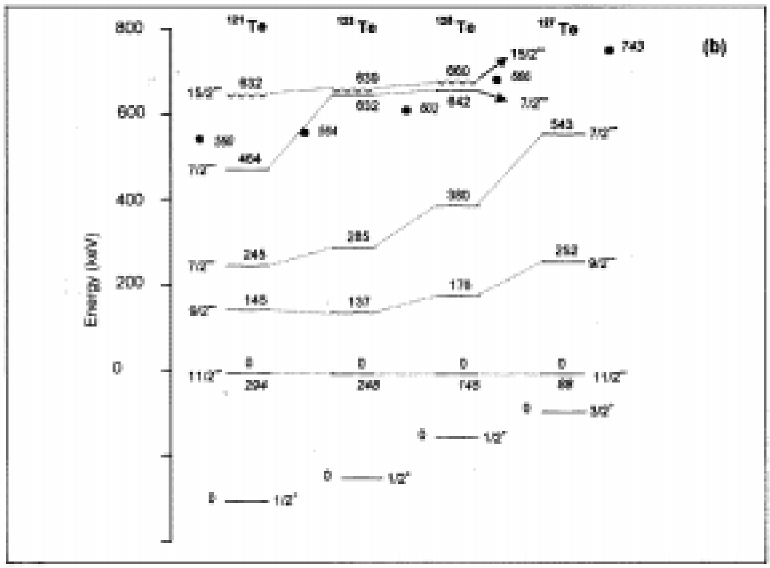

Figure 4(a, b). Experimental energy levels upto 1 MeV with assigned or indicated spin values in odd-A Te isotopes with $A = 121, 123, 125, 127$ for positive-parity levels in figure 4a and for the negative parity levels in figure 4b. In figure 4a, levels with uncertain spin values (3/2$^+$, 5/2$^+$), indicated from particle-transfer reaction studies or other arguments, are shown as ——— and levels with I = 7/2 are shown by wavy lines. The data is taken from the latest nuclear data sheets as compiled in the 1996 Table of Isotopes [2] supplemented by our results for ^{125}Te. In figure 4b, the level diagram is built on the 11/2$^-$ isomer whose excitation energy (in keV) is shown below the level (in italics) for each isotope; the corresponding ground state is shown lower at appropriate energy for each isotope. The relative energies (in keV), indicated above each level, are with respect to the 11/2$^-$ isomer energy taken as zero keV. The levels with I = 15/2 are shown by wavy lines. The quadrupole phonon energy, corresponding to the lowest 2$^+$ excitation energy (in keV) in the neighbouring even-A Te isotope, is shown by the symbol • in this figure and labelled in italics. We do not include in this figure levels with other spins, e.g. 13/2, 5/2, 3/2 etc., scattered around the quadrupole phonon energy.

figure 4b. The listed data are mainly taken from the adopted sets of the latest nuclear data sheets, as compiled in the 1996 Table of Isotopes [2], supplemented by our results and some other recent data [28].

First, we look at the systematics of positive parity states in figure 4a in the context of the 3 newly introduced levels, namely 402.0 keV 7/2$^+$, 538.6 keV 1/2$^+$, and 652.9 keV (3/2$^+$, 5/2$^+$) in ^{125}Te from our study. We find in figure 4a a low-lying 7/2$^+$ level both in ^{121}Te (443 keV) and ^{123}Te (490 keV); also a 7/2$^+$ level has been identified below 400 keV both in ^{117}Te and ^{119}Te, and around 455 keV in ^{129}Te. Taken together with our result, a low-lying 7/2$^+$ level at (400±100) keV has been identified in all the odd-A Te isotopes with $A = 117 - 129$, excepting in $A = 127$. Also, the 539 keV 1/2$^+$ level introduced by us in ^{125}Te fits in perfectly with the corresponding data for other isotopes. A trio of levels with $I^{\pi} = 3/2^{+}, 5/2^{+}, 7/2^{+}$ is seen above the 1/2^{+} level in all the 4 isotopes in figure 4a, supporting the existence of 653 keV level in ^{125}Te. It is of interest to note that, although there is almost a one-to-one correspondence in the observed level patterns of the 4 isotopes in figure 4a strongly supporting the occurrence of the 3 newly introduced levels in ^{125}Te, the observed level spectrum of ^{125}Te is seen to be considerably compressed in relation to its neighbours.

Turning our attention to the model description of the observed positive parity spectra, we note that the earliest attempt in this direction was the collective excitation model of deShalit [29]; in this picture, the excited states in the odd-A nucleus are generated by coupling the odd-particle (retained in the ground state) to the various excited states of the even–even core. Although the observed 443.6 keV 3/2^{+} and the 463 keV 5/2^{+} doublet may be considered to arise from the coupling of the 1/2^{+} ground state neutron to the 2^{+} (quadrupole) phonon of the core, the decay properties of these states do not agree with the predictions of the simple deShalit model. Kisslinger and Sorensen [30] investigated the spectra of odd-A spherical nuclei using the pairing-plus-quadrupole (PPQ) residual interaction in their quasiparticle formalism. However, as discussed by Walters and Myer [13], this approach had only a limited success even with the modification through permitting more higher vibrational components to mix into the lower-lying states. Extensive effort has been put in by several investigators [13,26,32–34] to understand these spectra using the quasiparticle–phonon coupling (QPC) model. In the QPC formalism, the 2^{+}_{1} state in the even-mass neighbour is taken as the quadrupole phonon which couples to the $s_{1/2}$ and $d_{3/2}$ quasiparticles leading to a doublet $(s_{1/2} \otimes 2^{+})_{3/2^{+},5/2^{+}}$ and a quartet $(d_{3/2} \otimes 2^{+})_{1/2^{+},3/2^{+},5/2^{+},7/2^{+}}$. Further, the core excitation process results in the appearance of $g_{7/2}$ and $d_{5/2}$ hole states (with $I^{\pi} = 7/2^{+}$ and $5/2^{+}$ respectively) in the medium energy spectrum. Prior to the present study, only 5 out of these 8 expected states had been identified. Our experimental identification of the 539 keV $1/2^{+}$ and the 653 keV $(3/2^{+})$ provides the missing states in the QPC picture. The newly added 133 keV gamma-ray, interconnecting the 672 keV 5/2^{+} and the 539 keV 1/2^{+} states, supports their QPC multiplet relationship. The observed decay patterns of the two 5/2^{+} states, as well as of the two higher 3/2^{+} states in figure 3, point to the admixture of these states arising respectively from the doublet and the quartet indicated earlier. The 5/2^{+} state with the $d_{5/2}$ hole configuration as its main component is not seen in this energy range. Detailed theoretical analysis of the spectroscopic data for odd-A Te isotopes by Sen [32] employed QPC formalism while incorporating both pairing effects and anharmonicity in the core vibrations. More recently, the Brasil group [33,34] have carried out similar calculations in the QPC and in the number-projected QPC formalism for the energy spectra and spectroscopic factors. Their calculations for Te isotopes with $A = 115 - 131$, 'using a parametrization taken from experimental data and from earlier calculations, without any adjustable parameter' provided only qualitative description leading to their concluding remark that the 'model can be considered as a good starting point for further theoretical calculations'. In their calculations, the lowest 3/2^{+} is placed around 140 keV (observed at 35 keV) and the 11/2^{-} isomer is predicted around 300 keV (observed at 144 keV); all other predicted positions also considerably overshoot the experiment. The observed compression of the ^{125}Te spectrum relative to its neighbours, pointed out earlier and also evident in figure 4a, remains the main stumbling block in any quantitative theoretical description.

Another significant approach for describing these positive parity states is the interacting boson–fermion model (IBFM). Fawwaz and Stewart [21] sought to describe the ^{125}Te spectrum in the IBFM by considering the coupling of a single fermion (neutron hole) to the ^{126}Te even–even core composed of five bosons. Considering the 4 positive parity orbitals, namely $s_{1/2}, d_{3/2}, d_{5/2}$ and $g_{7/2}$, they carried out successively one-, two-, three- and four-level calculations to conclude that their 3-level calculations 'agree best with observations'. Their calculated 3-level spectrum consists of three bands, the ground state band with 1/2, 3/2, 7/2, 5/2 sequence, a 3/2, 5/2, 7/2 sequence and the third band with 1/2, 3/2 sequence. Slightly varying the occupation probabilities, Fawwaz and Stewart [21] claimed a better fit with their (3b) calculations; in this set, they placed the 1/2$^+$ level at 670 keV whereas the presently known location of 1/2$^+$ is 539 keV; other band levels were predicted to lie above 700 keV. Our experimental results on the three new levels point to the preference for their (3a) calculations in so far as their predicted trio of $(3/2^+, 7/2^+, 5/2^+)$ levels around (430 $\pm$ 30) keV matches the experimentally observed trio of 402 keV 7/2$^+$, 443 keV 3/2$^+$ and 463 keV 5/2$^+$ levels from our study. However their higher levels again are too high to agree with the experiment. For instance the second 7/2$^+$ is predicted to lie around 800 keV, compared with the observed location around 640 keV.

Level systematics for the low-lying negative parity states is shown in figure 4b; in this figure we have indicated the level energies above each line relative to the 11/2$^-$ isomer (scaled as $E_x = 0$ with the isomer excitation energy, relative to the respective ground state shown lower), is listed in italics below the respective lines. The levels included in this figure are only those with spins 7/2, 9/2, 11/2 and 15/2 upto the relative excitation energy of around 800 keV. Also, we indicate in this figure, by a symbol (•) the experimental excitation energy of the lowest 2$^+$ state in the even–even neighbouring Te isotope. As mentioned earlier, $h_{11/2}$ is the only negative parity orbital embedded in the $N = 51 - 82$ domain which appears as a long-lived 11/2$^-$ isomer in all odd-A nuclei. In the QPC picture, we expect $(11/2^- \otimes 2^+)_{7/2,9/2,11/2,13/2,15/2}$ quintuplet located around the 2^+ phonon energy. As seen in figure 4b, experiments reveal a $15/2^-$ in all cases for $A = 117 - 125$ and also for $A = 129$ isotopes very close to the quadrupole phonon energy; a $13/2^-$ and also the second (not the lowest) excited $7/2^-$ is also seen [28] in the expected energy range in a few isotopes. However, an unexpectedly low-lying (320–470 keV) $9/2^-$ is observed in all the Te isotopes with $A = 117 - 129$. The experiments also reveal the lowest $7/2^-$ excitation energy (relative to the isomer) rising almost smoothly from 240 keV in ^{119}Te to 700 keV in ^{131}Te. The occurrence of these low-lying $9/2^-$ and $7/2^-$ states cannot be understood in the simple QPC picture. Sen [32] tried, albeit unsuccessfully, to explain this phenomenon by introducing a dipole–dipole term in the Hamiltonian. The extraordinary lowering of $I = j - 1$ states and $I = j - 2$ states, where j is a unique parity orbital, could be understood through cluster model calculations [31] which incorporate dressed $3qp$ and $5qp$ clusters. In this picture, discussed in detail by Rodland *et al* [27], these so-called anomalous coupling (AC) states are regarded as manifestations of $3qp$ and $5qp$ modes which, under the special shell structure conditions, may be regarded as 'elementary modes', breaking the QPC picture. Accordingly, the 321 keV 9/2$^-$ state is ^{125}Te is viewed as $3qp$ configuration. Additional support for this interpretation comes from the g-factor measurements [13]. The low-lying $7/2^-$ states in ^{123}Te and ^{125}Te respectively correspond to five particles and five holes in the $h_{11/2}$ shell. As remarked by Bondarenko *et al* [28] recently, in the context of their detailed study of negative parity states in ^{123}Te and ^{125}Te using radiative neutron capture, such 'anti-aligned' members with $I^\pi < 11/2^-$ of the $h_{11/2}$ family are anomalously compressed in energy with respect to the aligned $(I^\pi > 11/2^-)$ states. This anomalous descent of anti-aligned states, 'observed as a common feature of transitional nuclei in wide mass range', needs a deeper understanding of coupling mechanism.

4. Summary and conclusions

We have carried out precise measurements of the gamma-ray and conversion electron spectra following the ^{125}Sb decay. Precision of our data is established by comparing our results with the IAEA-adopted international calibration standards and other similar 'benchmark' measurements. A revised level scheme for ^{125}Te is constructed, based on summed energy rules for various loops, incorporating 37 gamma transitions; the latter include 13 transitions observed by us which are not listed in the adopted data set of the latest (1993) nuclear data sheets. Only one gamma ray (146 keV) from the NDS-93 adopted set does not appear in our measurements. The revised level scheme introduces three new levels at 402, 539 and 653 keV, with 10 (out of 13) new transitions connecting these levels with the earlier established levels. The 539 keV level, corresponding to the $I = 0$ peak reported in (d, t) reaction studies, is assigned $I^\pi = 1/2^+$. Taken together with an admissible $I^\pi = 3/2^+$ assignment for the 653 keV level and the other well-established levels, we now have the complete hextuplet corresponding to the $(s_{1/2} \otimes 2^+)_{3/2^+,5/2^+}$ and $(d_{3/2} \otimes 2^+)_{1/2^+,3/2^+,5/2^+,7/2^+}$ quasiparticle–phonon coupled states. Our studies reveal three $7/2^+$ levels in ^{125}Te including the closely spaced duo at 636 keV and 642 keV, and the newly introduced level at 402 keV. The latter is seen, in figure 4a, to fit smoothly in the level systematics of the odd-A Te isotopes. Theoretically, the IBFM description places the lowest $7/2^+$ of the ground band in this vicinity; the $(3/2^+, 7/2^+, 5/2^+)$ trio of predicted levels matches the observed spectra. The QPC calculations [33] also predict this trio of states, including a low-lying $7/2^+$, well below the $1/2^+$ level; however, in these calculations, the whole spectrum is shifted upwards possibly due to the input *qp* energies. QPC calculations also predict a large spacing between the two $7/2^+$ levels. No theoretical description admits of two very closely spaced $7/2^+$ levels. Understanding the structure of these $7/2^+$ levels in ^{125}Te is thus a challenging open question. Another new feature revealed in our systematics study, which needs fresh theoretical inputs, is the relatively compressed positive parity spectrum of ^{125}Te. The low-lying negative parity $9/2^-$ and $7/2^-$ levels are, on the other hand, described as the $(h_{11/2})^3$ and $(h_{11/2})^{-5}$ structures respectively; alternatively, these two levels may correspond to the anomalously descended 'anti-aligned' states of the $h_{11/2}$ family. It is expected that the presently reported more extensive gamma ray and conversion electron data and the revised low-energy level scheme of ^{125}Te, taken together with the results from reaction studies, provides a better data base for understanding the level structures in transitional nuclei.

Acknowledgement

Valuable help from B Singh during the course of these investigations is gratefully acknowledged.

References

[1] J Katakura, M Oshima, K Kitao and H Iimura, *Nucl. Data Sheets* **70**, 217 (1993)

[2] R B Firestone and V S Shirley (eds), *Table of Isotopes*, 8th ed. (John Wiley and Sons, Inc., New York, 1996)
[3] G Friedlander, M Goldhaber and G Scharff-Goldhaber, *Phys. Rev.* **74**, 981 (1948)
[4] R S Narcisi, A.E.C.U. Report 4336 (1958)
[5] G Chandra and V R Pandharipande, *Nucl. Phys.* **46**, 119 (1963)
[6] K C Mann, F A Payne and R P Chaturvedi, *Can. J. Phys.* **42**, 1700 (1964) and references therein
[7] E P Mazets and Y V Sergeenkov, *Izv. Akad. Nauk SSSR. Ser. Fis.* **30**, 1185 (1966); *Bull Acad. Sci. USSR. Phys. Ser.* **30**, 1237 (1967)
[8] N J Stone, R B Frankel and D A Shirley, *Phys. Rev.* **172**, 1243 (1968)
[9] T Inamura, *J. Phys. Soc. Jpn.* **24**, 1 (1968)
[10] G Ardisson, K Johansson and E Karlson, *Nucl. Phys.* **A154**, 369 (1970)
[11] T S Nagpal and R E Gaucher, *Can. J. Phys.* **48**, 2978 (1970)
[12] J B Gupta, N C Singhal and J H Hamilton, *Z. Phys.* **261**, 137 (1973)
[13] W B Walters and R A Meyer, *Phys. Rev.* **C14**, 1925 (1976)
[14] R J Gehrke, R G Helmer and R C Greenwood, *Nucl. Instrum. Methods* **147**, 405 (1977)
[15] R Prasad, *Czech. J. Phys.* **B29**, 737 (1979)
[16] K Singh and H S Sahota, *Indian J. Pure Appl. Phys.* **21**, 19 (1983)
[17] Y Iwata, M Yasuhara, K Maeda and Y Yoshizawa, *Nucl. Instrum. Methods* **219**, 123 (1984)
[18] L Longoria-Gandara, M U Rajput and T D Mac Mahon, *Nucl. Instrum. Methods* **A286**, 529 (1990)
[19] R G Helmer, *Appl. Radiat. Isot.* **41**, 75 (1990)
[20] D Smith, D H Woods, S A Woods, J L Makepeace, R E Mercer and C W A Downey, *Nucl. Instrum. Methods* **A312**, 353 (1992)
[21] N I Fawwaz and N M Stewart, *J. Phys.* **G19**, 113 (1993)
[22] J Goswamy, B Chand, D Mehta, N Singh and P N Trehan, *Appl. Radiat. Isot.* **42**, 1025 (1991)
[23] A Kerek, J Kownacki and A Marelius, *Nucl. Phys.* **A194**, 64 (1972)
[24] J Barrette, M Barrette, R Haroutunian, G Lamoureux, S Monaro and S Markiza, *Phys. Rev.* **C11**, 282 (1975)
[25] M A G Fernandes and M N Rao, *J. Phys.* **G3**, 1397 (1977)
[26] T Rodland, J S Vaagen and J R Lien, *Nucl. Phys.* **A338**, 13 (1980)
[27] T Rodland, J R Lien, J S Vaagen, G Lovhoiden and C Ellegaard, *Phys. Scr.* **29**, 529 (1984)
[28] V Bondarenko, J Honzatko and I Tomandl, *Z. Phys.* **A354**, 235 (1996)
[29] A deShalit, *Phys. Rev.* **122**, 1500 (1961)
[30] L S Kisslinger and R A Sorensen, *Rev. Mod. Phys.* **35**, 74 (1963)
[31] A Kuriyama, T Marumori and K Matsuyanagi, *Prog. Theor. Phys.* **58**, 53 (1975)
[32] S Sen, *J. Phys.* **G1**, 286 (1975)
[33] H Dias and L Losano, *Phys. Rev.* **C50**, 1377 (1994)
[34] C A P Ceneviva, L Losano and H Dias, *Int. J. Mod. Phys.* **E4**, 419 (1995)
[35] *"X-ray and gamma-ray standards for detector calibration"*, IAEA Coordinated Research Programme Report No IAEA-TECDOC-619 (1991)
[36] M Sainath, K Venkataramaniah and P C Sood, *Phys. Rev.* **C56**, 2468 (1997)
[37] M Sainath and K Venkataramaniah, *Nuovo Cimento* **A111**, 223 (1998)
[38] M Sainath, K Venkataramaniah and P C Sood, *Phys. Rev.* **C58**, 3730 (1998)
[39] V Petkov and N Bakaltchev, *J. Appl. Cryst.* **23**, 138 (1990)
[40] R S Hager and E C Seltzer, *Nucl. Data Sheets* **A4**, 1 (1968)